Challenge Journal of Structural Mechanics

Research Article

Optimum parameters for adjacent structures coupled by fluid viscous dampers considering soil–structure interaction

Oğuz Akın Düzgün [a,*], Yavuz Selim Hatipoğlu [b], Osman Ünsal Bayrak [a]

[a] *Department of Civil Engineering, Atatürk University, 25240 Erzurum, Türkiye*
[b] *Department of Civil Engineering, Bayburt University, 69000 Bayburt, Türkiye*

ABSTRACT

In this paper, the optimum conditions which ensure that the resulting minimum base shear force and minimum roof displacement for two adjacent frame structures interconnected by fluid viscous dampers, including soil-structure interaction (SSI) effects under seismic excitation were presented. A two-dimensional (2D) finite element analysis was carried out with the Taguchi method. As non-reflecting boundaries, viscous boundary conditions were used on the edges of finite soil region. An optimization study was carried out for four parameters such as soil type, height ratio of the frames, damping coefficient of viscous damper, and the location of the viscous damper each with four levels. The optimum conditions which minimize maximum roof displacements and the maximum base shear forces have been obtained. The most affecting parameter on the system response was found to be soil type. It was also found that the sufficient damping coefficient of the viscous damper is equal to $1x10^5$ N.s/m for minimum response. The minimum system response can be achieved by using only one damper. It can be drawn that the Taguchi method can be used with the finite element (FE) method for determining optimum conditions of a soil-structure system for minimum system response.

ARTICLE INFO

Article history:
Received 12 September 2022
Revised 31 October 2022
Accepted 18 November 2022

Keywords:
Adjacent frames
Fluid viscous dampers
Soil-structure interaction
Optimum conditions
Taguchi method

1. Introduction

Vibrations due to several reasons like earthquake excitations, machine foundations, heavy traffic, blasting, or strong wind can cause damage to structures and annoyance to residents. The effect of such vibrations can be mitigated or prevented by implementing vibration control systems in structures. The main purpose of such systems is to provide additional damping to the structures by either transmitting it directly to any connected structure or converting energy to heat (Bhaskarao and Jangid 2006a; Patel and Jangid 2014). Coupling neighboring structures with suitable energy dissipation devices is an effective and practical approach to get some advantages such as avoiding pounding and response reduction (Bhaskarao and Jangid 2006a; Bharti et al. 2010). Vibration control systems may be divided into four categories such as active, passive, semi-active, and hybrid systems according to their energy consumption (Housner et al. 1997; Zhu et al. 2001). However, employing passive energy absorbers is the most common way of adding damping to structures when considering their simplicity in design, operation, and maintenance (Bakre and Jangid 2007; Patel and Jangid 2014). There are various types of passive energy-absorbing devices. One of them is viscous dampers. A typical viscous damper is usually composed of a piston in the damper housing filled with viscous material in the form of either solid (rubber or acrylics) or fluid (silicone or oil). One of the viscous damper types is fluid viscous dampers. In a fluid viscous damper, the energy is dispersed by the movement of the piston in the viscous fluid. It is considered that the output force of the viscous damper is in direct proportion to the velocity of the piston (Makris and Constantinou 1990; Housner et al. 1997; Patel and Jangid 2014).

* *Corresponding author*. Tel.: +90-442-231-4771 ; Fax: +90-442-231-4910 ; E-mail address: oaduzgun@atauni.edu.tr (O. A. Düzgün)
ISSN: 2149-8024 / DOI: https://doi.org/10.20528/cjsmec.2023.01.002

Numerous studies have been carried out on the dynamic response of adjacent structures interconnected by different energy-dissipating devices. Westermo (1989), one of the pioneering works on the subject, examined the effectiveness of hinged links for adjacent structures to avoid pounding damages. The effectiveness of viscous dampers on the system response of adjacent coupled structures under dynamic excitation was studied by Luco and De Barros (1998), Xu et al. (1999), Bhaskararao and Jangid (2007), Cimellaro and Garcia (2007), Tubaldi et al. (2014), Tubaldi (2015), Wu et al. (2017), and De Domenico et al. (2019). These studies indicated that response reduction and avoiding mutual pounding can be achieved by coupling adjacent structures with viscous dampers. In addition, the number and location of the dampers affect the dynamic behavior of coupled structures. Apart from these issues, optimum locations of dampers for response mitigation (Luco and De Barros 1998; Bhaskararao and Jangid 2006b; De Domenico et al. 2019), optimum damping coefficient of damper (Xu et al. 1999; Zhu and Xu 2005; Bhaskararao and Jangid 2007; Wu et al. 2017; De Domenico et al. 2019), and effective damping coefficient of fluid viscous dampers (FVDs) for dynamic response mitigation (Düzgün and Hatipoğlu 2022) were also studied. It is well known that considering the mechanical properties of soil medium in the modeling and analysis is considerably affected the dynamic behavior of structures. However, studies on coupled adjacent buildings that considering soil-structure interaction (SSI) are quite limited. The effects of geotechnical properties of soil on the dynamic response of adjacent buildings interconnected by dampers were studied by Patel and Jangid (2008), Zou et al. (2012), and Avinash et al. (2017). In these studies, the problem was handled in a simplified manner probably due to the complexity of the problem. It is clear that there is a need to conduct more studies on the dynamic response of coupled adjacent buildings including SSI effects to get a better understanding of the effects of the soil medium on coupled system response.

In the conventional design of experiments, increasing the number of variables leads to increasing the number of experiments. Hence, more material, money, time, and personnel are necessary for the conventional experiment design. Therefore, researchers have tried to develop methods to reduce the number of experiments without any data loss. The Taguchi method is a statistical method developed by Taguchi (1960) to investigate the effects of different parameters on determining the optimum operating conditions of any process. Optimization of the process is carried out with the design of the experiment tool using an orthogonal array, which is formed according to parameters and their levels. This method computes the optimum conditions according to the analysis of variance using obtained data. However, the optimum condition is a point estimation. Therefore, the result of the optimum condition should be controlled with an error ratio whether it is in a certain confidence interval. Moreover, the most effective parameter or the influence rank of the parameters can be determined by the Taguchi method too (Bayrak and Hınıslıoğlu 2017).

The goal of this study is to determine the parameters such as soil type, height ratio of the structures, damping coefficient of damper, and the location of the damper which ensure that the resulting minimum base shear force and minimum roof displacement for two adjacent multi-story frame structures interconnected by FVDs, including SSI effects under earthquake excitation by finite element (FE) method. Viscous boundary conditions were used as special non-reflecting boundaries on the edges of finite soil region. Since the dynamic response of the system is affected by many factors and different solutions, the FE analyses were carried out with the Taguchi method which is a special design of experiment. As a result of the study, the optimum conditions were determined for the minimum roof displacements and minimum base shear forces of the coupled structures-soil system.

2. The Taguchi Method

The Taguchi method is a mighty tool to use to investigate the effects of different parameters on determining the optimum conditions of any process. In this method, more information can be obtained by using lesser data (Taguchi 1960). An orthogonal array technique was used in order to design the finite element analyses (FEA) (Taguchi 1960). Factors and their levels that affect the roof displacements and the base shear forces of two adjacent structures were decided according to the former studies on the subject. The selected factors and their levels given in Table 1 were used in the FEA according to the L_{16} orthogonal array which is recommended by Taguchi (1960) for four factors each has four levels (Table 2) (Taguchi 1960; Bayrak and Hınıslıoğlu 2017).

Table 1. Factors and their levels used for FEA.

Factors	Levels			
	1	2	3	4
(A) Soil Type	-	I	II	III
(B) H_B/H_A Ratio	1.00	1.50	1.75	2.00
(C) Damping Coefficient (Ns/m)	1×10^4	1×10^5	1×10^6	1×10^7
(D) Number of Damper	1 FVD	3 FVD	6 FVD	12 FVD

Table 2. L_{16} orthogonal array.

FEA No	Soil Type	H_B/H_A Ratio	Damping Coefficient	Number of Damper
1	1	1	1	1
2	1	2	2	2
3	1	3	3	3
4	1	4	4	4
5	2	1	2	3
6	2	2	1	4
7	2	3	4	1
8	2	4	3	2
9	3	1	3	4
10	3	2	4	3
11	3	3	1	2
12	3	4	2	1
13	4	1	4	2
14	4	2	3	1
15	4	3	2	4
16	4	4	1	3

The numbers shown in Table 2 are the levels of each factor. The analysis order was arbitrarily chosen to minimize the noise sources that affect the results in a negative way (Taguchi 1960; Bayrak and Hınıslıoğlu 2017). The obtained roof displacements and base shear forces were calculated based on the quality characteristic of 'smaller the better' using Eq. (1):

$$\frac{S}{N} = -10\log_{10}\left(\frac{1}{n}\sum_{i=1}^{n} Y_i^2\right) \tag{1}$$

where S/N (signal to noise ratio, unit: dB) are performance statistics, Y_i is a performance value of the i^{th} analysis, and n is the number of repeated analysis.

The optimum conditions can be obtained by the levels of factors that maximize the average S/N values. However, in the Taguchi method, the levels of factors indicating optimum conditions may not be found in L_{16} orthogonal array (Table 2) (Bayrak and Hınıslıoğlu 2017). In such cases, the prediction of the S/N value for optimum conditions can be calculated by Eq. (2) according to the L_{16} orthogonal array.

$$Y_i = \mu + X_i + e_i \tag{2}$$

where X_i, μ, and e_i are the fixed effect of the factor level combination used in the i^{th} analysis, the overall mean of the performance value, and the random error in the i^{th} analysis, respectively (Taguchi 1960). Because of Eq. (2) is a point estimation, the confidence interval must be evaluated. The confidence interval at the chosen error level may be calculated by using Eq. (3).

$$\mu \pm \sqrt{F_{\alpha,1,DF_{MSe}}\left[\left(\frac{1+m}{N}\right)+\left(\frac{1}{n_i}\right)\right]} \tag{3}$$

where α, F, DF_{MSe}, N, m, and n_i are the error level, the value of the F table, degrees of freedom of mean square error, the number of total analyses, degrees of freedom used in the prediction of Y_i, and the number of repeated analysis, respectively.

3. Numerical Modeling of Coupled System

First of all, some assumptions and limitations were considered in order to make the problem governable. Two adjacent structures were assumed to be symmetric frames with their symmetric planes in alignment. Possible torsional effects due to linked viscous dampers between two structures were neglected. Assuming the ground excitation occurred in one dimension in the plane of the structures, the problem can be handled as a two-dimensional (2D) problem. The adjacent frame structures were idealized as linear shear-type structures with lateral degrees of freedom at their floor levels. The adjacent structures system was assumed to remain in the linear elastic stage under ground motion due to a considerable increase in energy-absorbing capacity. It was also assumed that the floors of each frame were at the same level where two neighboring floors were connected with fluid viscous dampers. However, the number of stories in each structure can be different. Each viscous damper was modeled as a linear dashpot direct proportional to the relative velocity between the two adjacent floors. Both adjacent structures were assumed to be subjected to the same seismic excitation and the effects due to SSI were considered. The soil was assumed to be homogeneous, linear-elastic, and isotropic medium.

The coupled structures-soil model presented in this study is schematically shown in Fig. 1. Structure A and

Structure B were assumed that have n stories and n + m stories, respectively. The mass, damping coefficient and lateral stiffness values for i^{th} story are $m_{i,A}$, $c_{i,A}$, and $k_{i,A}$ for Structure A and $m_{i,B}$, $c_{i,B}$, and $k_{i,B}$ for Structure B, respectively. The damping coefficient of the viscous damper at i^{th} floor is $c_{d,i}$. The governing equations of motion of the interconnected structures system can be expressed in the matrix form as (Xu et al. 1999; Zhang and Xu 1999):

$$\mathbf{M}\ddot{\mathrm{U}} + (\mathbf{C} + \mathbf{C_D})\dot{\mathrm{U}} + (\mathbf{K} + \mathbf{K_D})\mathrm{U} = -\mathbf{M}\,\mathbf{I}\,\ddot{u}_g \tag{4}$$

where, M, C and K are the mass, damping and stiffness matrices of the system, respectively. K_D and C_D represent the additional damping and stiffness matrices due to the installation of the FVDs, respectively. The corresponding equations of motions, when the two adjacent buildings are connected with viscous dampers, can simply be obtained by making K_D equal to null matrix in the Eq. (4) (Bhaskararao and Jangid 2004). U is the relative displacement vector with respect to the ground motion; I is a vector with all elements equal to 1, and $\ddot{u}_g$ is the applied ground motion acceleration. The details of each matrix were given in (Xu et al. 1999; Zhang and Xu 1999; Bhaskararao and Jangid 2004).

A number of dynamic analyses were carried out by the finite element-based software ANSYS (2021) according to the L_{16} orthogonal array presented in Table 2. The direct approach which enables the solving of the coupling frames system and the soil in a single step was employed. The columns and beams of the frames were modeled with BEAM189 element (ANSYS 2021) which is a quadratic three-node beam element. The structural elements were idealized as the linear-elastic materials with Rayleigh damping. The damping ratio (ξ) of structures is assumed to be 0.05 (Ada and Ayvaz 2019). Rayleigh damping is a linear combination of the mass and stiffness matrices, and it can be calculated by the following equation:

$$\mathbf{C} = \alpha[\mathbf{M}] + \beta[\mathbf{K}] \tag{5}$$

where α and β are the damping coefficients with units $1/s$ and s, respectively. If the damping coefficients are not known, assuming the i^{th} and j^{th} modes have the same damping ratio (ξ), the coefficient can be calculated by the following equation:

$$\begin{Bmatrix}\alpha\\ \beta\end{Bmatrix} = \frac{2\xi}{\omega_i+\omega_j}\begin{Bmatrix}\omega_i\omega_j\\ 1\end{Bmatrix} \tag{6}$$

where ω_i and ω_j are the angular frequencies of the i^{th} and j^{th} modes, respectively.

The soil environment assumed to be a homogeneous, isotropic, and linear-elastic material was modeled with PLANE182 element (ANSYS 2021) which is a four-node plane element with three degrees of freedom at each node. In order to provide energy transmitting in boundaries, viscous boundary conditions were defined at the edges of finite soil medium by using COMBIN14 element (ANSYS 2021) in both vertical and horizontal directions. Viscous boundary conditions were used as non-reflecting boundaries on the edges of finite soil zone.

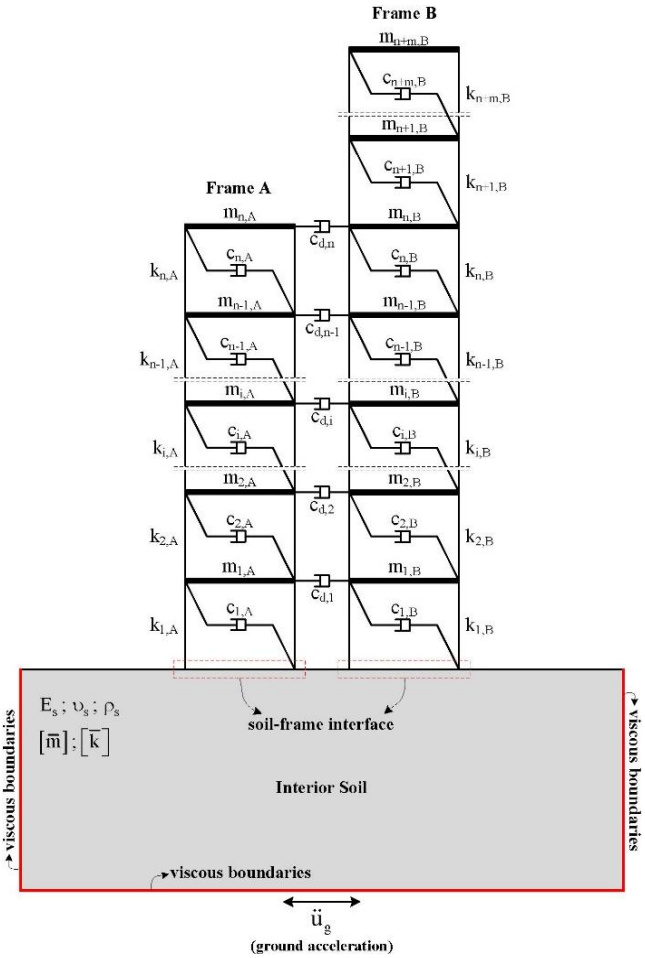

Fig. 1. Schematic representation of adjacent structures-soil system (Düzgün and Hatipoğlu 2022).

The non-reflecting viscous boundaries was first introduced by Lysmer and Kuhlemeyer (1969). Since its implementation involves placing viscous dashpots at the boundary, it is also often referred to as the viscous boundary. Viscous boundary method appears to treat both dilatational and shear waves with sufficient accuracy in many applications. The viscous forces, or dashpots, do not depend upon the frequencies of the transmitted waves. It can absorb harmonic and non- harmonic waves. Viscous boundaries are local in space and time; therefore, this technique is suitable for transient analysis (Wolf 1988).

Fluid viscous dampers, as an energy dissipating device, were used for avoiding pounding and response reduction in adjacent frames. The linear damper behavior can be expressed by

$$F_T = F_D + F_E = CV^{c.exp} + KD_k \tag{7}$$

where, F_T, V, C, K, and D_k are total force provided by the damper, velocity across the damper, the damping coefficient, the spring constant, and displacement across the spring, respectively. The damping exponent expressed by *c.exp* and it must be positive. In the literature, the practical range of the damping exponent is between 0.3 and 2 (Tezcan and Uluca 2003; Hou 2008; Uz 2009). In this study, since the fluid viscous dampers were taken as

linear, the damping exponent was assumed equal to 1. F_T consists of two parts as shown in Eq. (7). The first part is the damping force F_D and the second part is restoring force F_E. In the lack of stiffness, the force in the fluid viscous damper can be expressed by

$$F_D = CV^{c.exp}\text{sgn}(V) \quad (8)$$

where, sgn is the signum function. Then, the function defines the sign of the relative velocity term (Hou 2008). The verification of the model was presented in Düzgün and Hatipoğlu (2022).

4. Parametric Studies

In the soil-adjacent structures system, the mass density, modulus of the elasticity, and Poisson ratio of the adjacent structures were assumed to be ρ_{str}=2500 kg/m^3, E_{str}=30000 MPa, and υ=0.20, respectively. The mean story-to-story spacing was 3 m. It was assumed that the height of Structure A (H_A) was constant as 36 meters (12-story) while the height of Structure B (H_B) was selected proportional to H_A. The H_B/H_A ratios used in this study can be seen in Table 1. On the other hand, the column and beam dimensions of both frames were the same for each story with the column dimensions of 0.5x0.5 m, and the beam dimensions of 0.3x0.6 m. The damping ratio of both adjacent frames was taken constant as 5%. The mass and shear stiffness of both frames were uniform for each story with the mass of 1.124x10^4 kg, and the shear stiffness of 2.1x10^8 N/m. Fluid viscous dampers were used to connect two adjacent floors. Four different damper connection scenarios are taken based on the number of dampers as can be seen in Table 1. The damper connection scenarios are shown in Fig. 2. The selected damping coefficients for the dampers are also shown in Table 1.

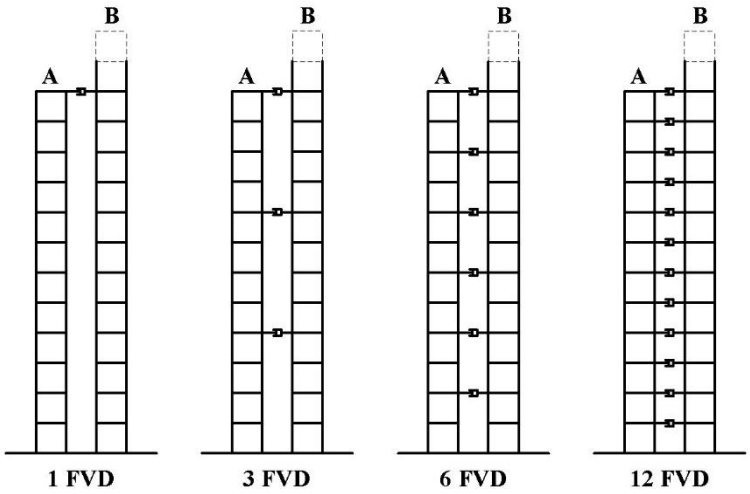

Fig. 2. Fluid viscous damper connection scenarios.

It is noted that no relative displacement was allowed at the soil-frame interface in all simulations. The dimensions of finite soil region were selected as 210 m. in width and 90 m. in depth. In order to obtain dynamic response of adjacent structures-soil system, three different soil types were considered by the name of Soil Type I Soil Type II and Soil Type III. These soil types represent dense, medium, and loose soil characteristics, respectively. The selected mechanical properties of all soil types are presented in Table 3. The mechanical properties of all soil types were adopted from the study conducted by Çelebi et al. (2012). The mechanical properties of selected soil types represent the general properties of the loose, medium, and dense soils instead of representing a specific soil material to determine how to affect soil medium the dynamic response of adjacent frames.

Kocaeli, Turkey (1999) earthquake (PGA = 0.34g) was chosen for acceleration data of the ground motion acting horizontally at the bottom edge of the soil layer. The ground motion time history is shown in Fig. 3. A numerical procedure was used to evaluate the system response in the analyses. The finite elements and boundary conditions mentioned earlier were used in the numerical treatment.

Table 3. Mechanical properties of soil types.

Soil Type	I	II	III
Modulus of Elasticity (E) (MPa)	6000	400	35
Poisson Ratio (υ)	0.30	0.30	0.25
Mass Density (ρ) (kg/m^3)	2100	1900	1700
Shear Wave Velocity (v_s) (m/sec)	1029	285	91
Pressure Wave Velocity (v_p) (m/sec)	2141	532	157

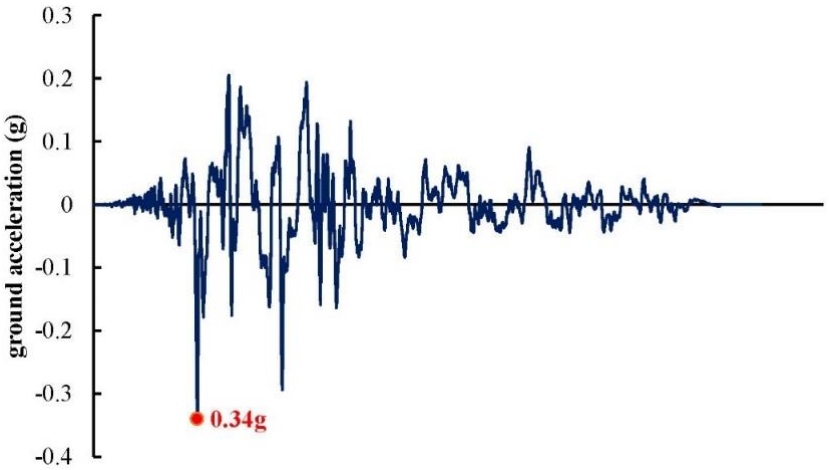

Fig. 3. Input ground motion time history.

5. Results and Discussion

According to the factors and levels (Tables 1 and 2), the optimum conditions were determined for the minimum roof displacements and minimum base shear forces of the coupled structures-soil system by using the Taguchi method. The results were presented separately for the Structures A and B. The S/N values were calculated by using Eq. (1) according to the FE analysis results given in Table 4. The optimum conditions for the minimum response are obtained by average S/N effects which can be calculated from the S/N values.

Table 4. The S/N values, roof displacement and base shear force values of both frames.

	Performance Statistics (S/N)							
	Structure A				Structure B			
	Roof Displacements		Base Shear Forces		Roof Displacements		Base Shear Forces	
FEA No	S/N	m	S/N	kN	S/N	m	S/N	kN
1	20.193	0.0978	-45.251	183.04	20.193	0.0978	-45.251	183.04
2	22.225	0.0774	-43.495	149.53	17.380	0.1352	-43.236	145.14
3	20.336	0.0962	-44.366	165.31	14.789	0.1822	-42.985	141.01
4	15.274	0.1723	-47.064	225.53	8.232	0.3876	-46.940	222.34
5	21.190	0.0872	-44.899	175.78	21.577	0.0834	-50.447	332.92
6	20.193	0.0978	-44.674	171.28	15.815	0.1619	-45.351	185.16
7	17.822	0.1285	-45.350	185.13	12.822	0.2285	-46.008	199.70
8	17.247	0.1373	-45.978	199.02	9.042	0.3531	-44.975	177.32
9	11.434	0.2681	-51.995	397.89	11.444	0.2678	-52.895	441.33
10	13.073	0.2220	-48.671	271.37	9.704	0.3272	-48.974	280.99
11	10.958	0.2832	-51.412	372.06	6.630	0.4661	-51.157	361.28
12	14.600	0.1862	-48.102	254.15	8.702	0.3672	-47.143	227.59
13	10.377	0.3028	-46.836	219.69	10.377	0.3028	-47.744	243.88
14	10.308	0.3052	-45.829	195.63	6.335	0.4822	-45.618	190.95
15	10.288	0.3059	-46.844	219.89	3.129	0.6975	-44.869	175.17
16	7.004	0.4465	-47.344	232.91	-4.420	1.6634	-49.591	301.69
Average	15.158		-46.757		10.734		-47.074	

Table 5. The average S/N effects for roof displacements of Structure A.

Factors	Levels			
	1	2	3	4
(A) Soil Type	19.507	19.113	12.516	9.494
(B) H_B/H_A Ratio	15.799	16.450	14.851	13.531
(C) Damping Coefficient	14.587	17.076	14.831	14.137
(D) Number of Damper	15.731	15.202	15.401	14.297

Table 6. The average S/N effects for roof displacements of Structure B.

Factors	Levels			
	1	2	3	4
(A) Soil Type	15.149	14.814	9.120	3.855
(B) H_B/H_A Ratio	15.898	12.309	9.343	5.389
(C) Damping Coefficient	9.555	12.697	10.403	10.284
(D) Number of Damper	12.013	10.857	10.284	9.655

Table 7. The average S/N effects for base shear forces of Structure A.

Factors	Levels			
	1	2	3	4
(A) Soil Type	-45.044	-45.225	-50.045	-46.713
(B) H_B/H_A Ratio	-47.245	-45.667	-46.993	-47.122
(C) Damping Coefficient	-47.170	-45.835	-47.042	-46.980
(D) Number of Damper	-46.133	-46.930	-46.320	-47.644

Table 8. The average S/N effects for base shear forces of Structure B.

Factors	Levels			
	1	2	3	4
(A) Soil Type	-44.603	-46.695	-50.042	-46.956
(B) H_B/H_A Ratio	-49.084	-45.795	-46.255	-47.162
(C) Damping Coefficient	-47.838	-46.424	-46.618	-47.417
(D) Number of Damper	-46.005	-46.778	-47.999	-47.514

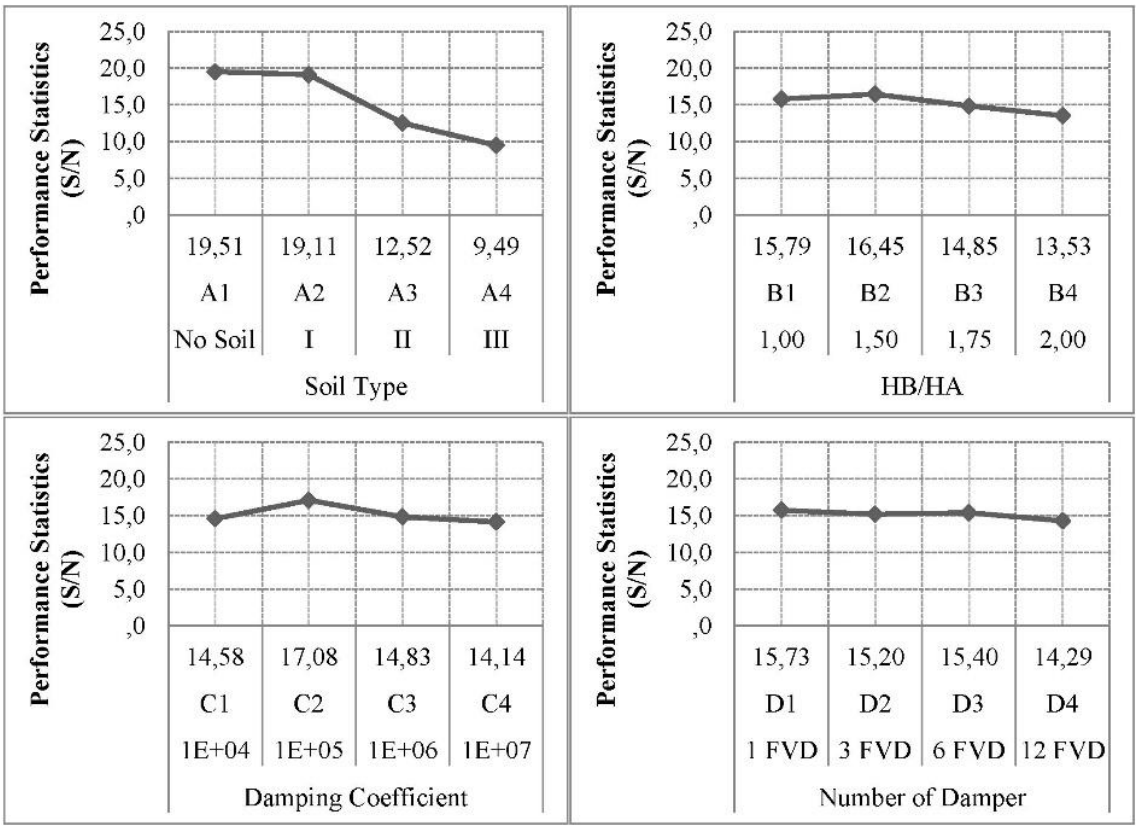

Fig. 4. The effects of parameters on roof displacements for Structure A.

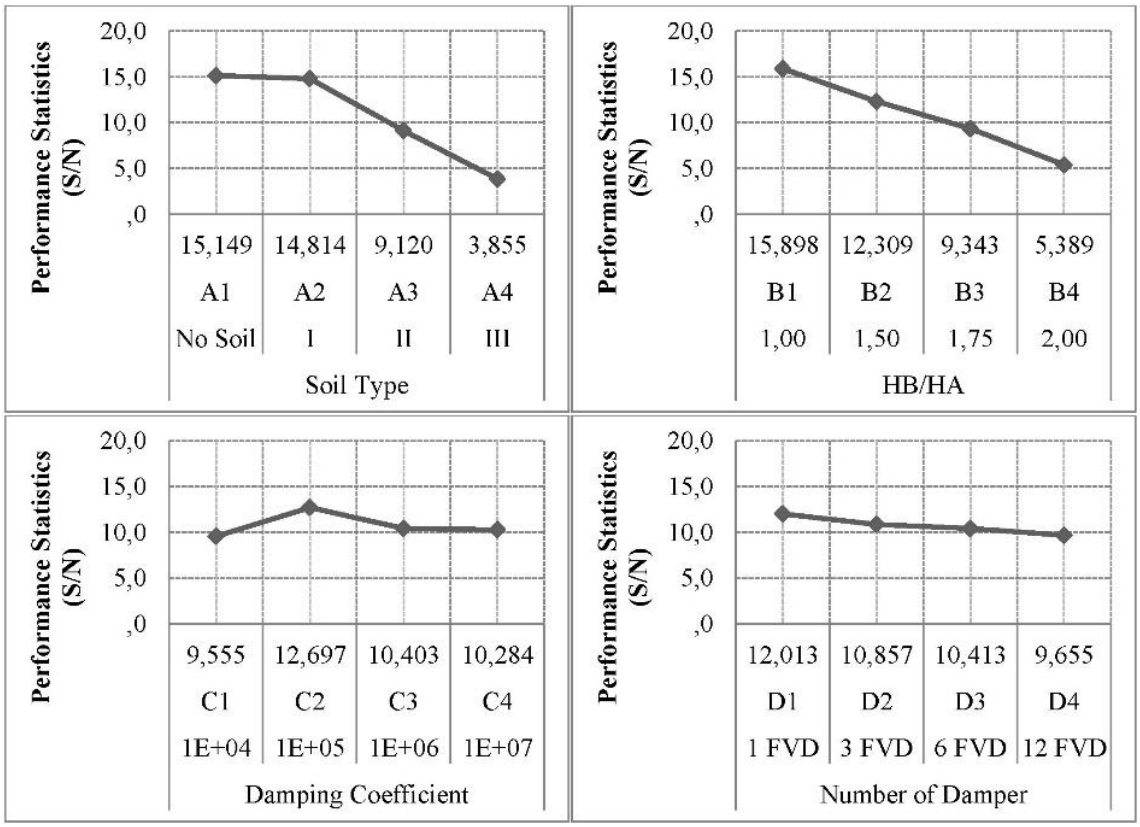

Fig. 5. The effects of parameters on roof displacements for Structure B.

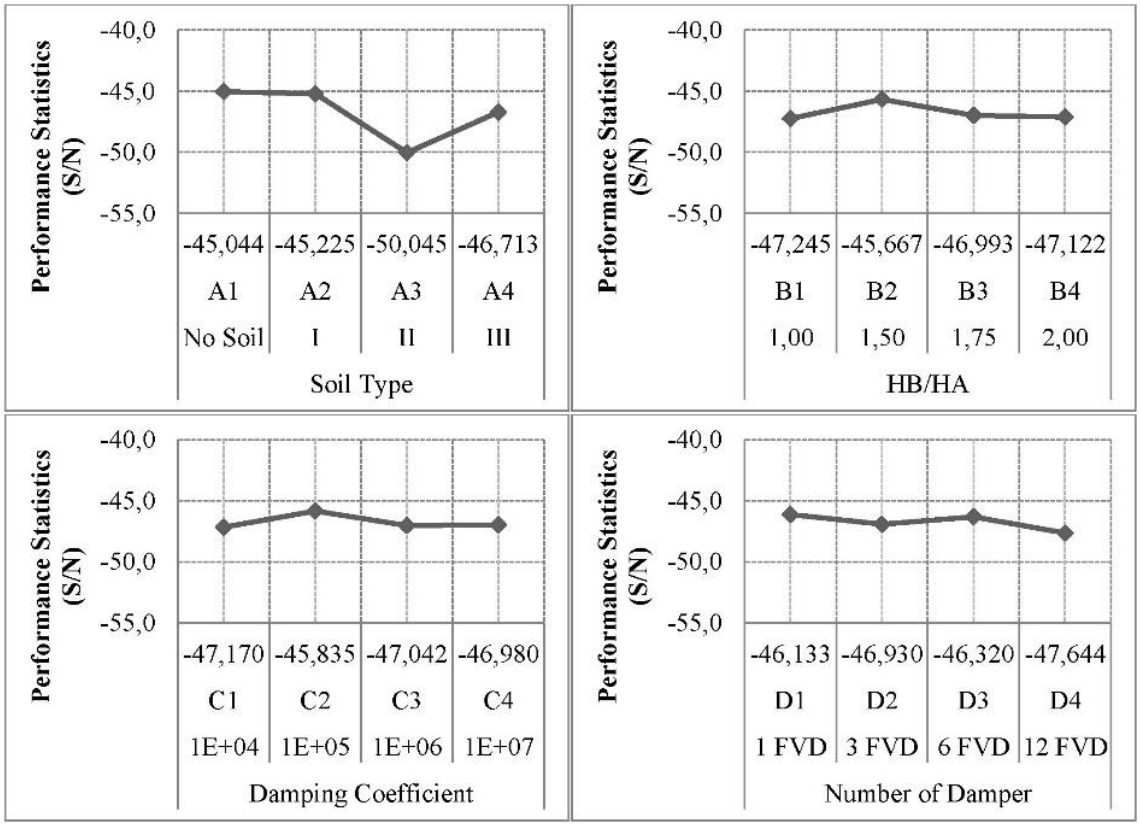

Fig. 6. The effects of parameters on base shear forces for Structure A.

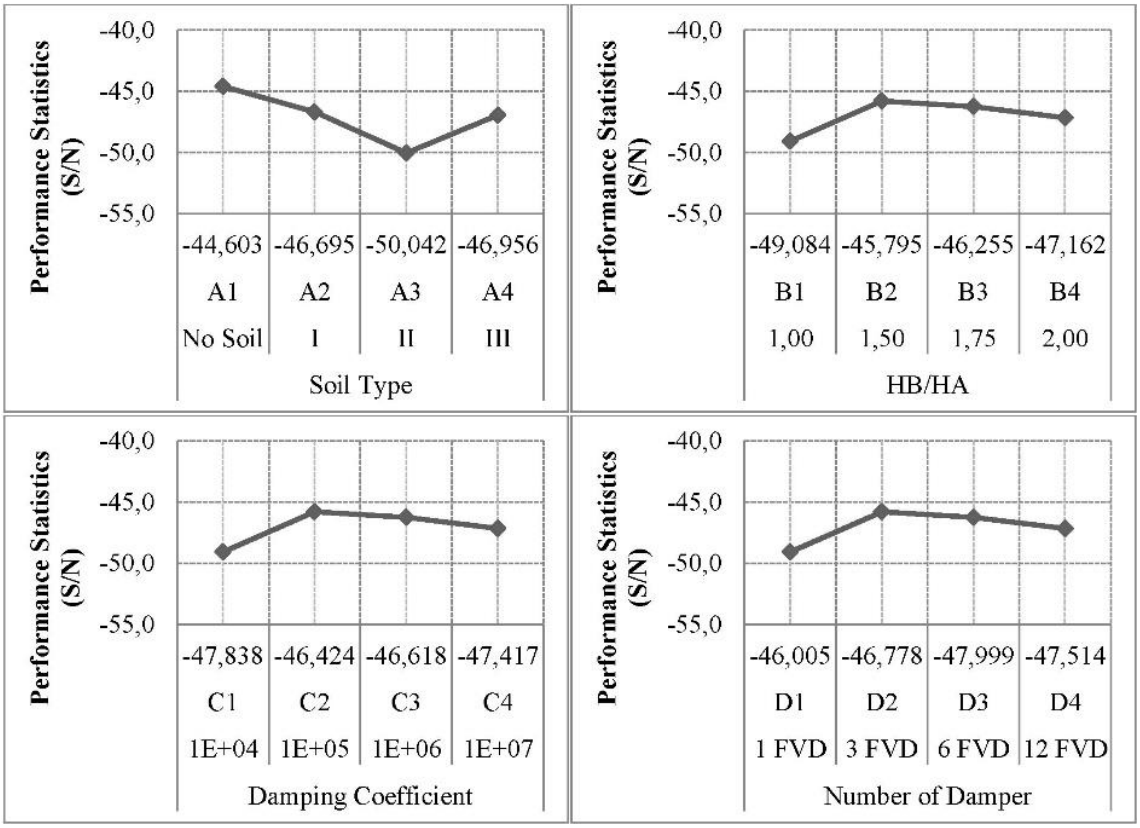

Fig. 7. The effects of parameters on base shear forces for Structure B.

Table 9. Contribution of the factors on the roof displacements of Structure A.

Factors	Level No	Contribution to the S/N
Soil Type	A1	4.349
H_B/H_A Ratio	B2	1.292
Damping Coefficient	C2	1.918
Number of Damper	D1	0.573
Contribution of all factors		8.132
Expected value (S/N) / (m)		23.290 / 0.068
Confirmation result (S/N) / (m)		21.618 / 0.083
Confidence interval (α=95%) (S/N)		19.946 – 26.634

Table 10. Contribution of the factors on the roof displacements of Structure B.

Factors	Level No	Contribution to the S/N
Soil Type	4.415	4.349
H_B/H_A Ratio	5.164	1.292
Damping Coefficient	1.963	1.918
Number of Damper	1.279	0.573
Contribution of all factors		12.821
Expected value (S/N) / (m)		23.555 / 0.066
Confirmation result (S/N) / (m)		20.175 / 0.098
Confidence interval (α=95%) (S/N)		18.658 – 28.452

Table 11. Contribution of the factors on the base shear forces of Structure A.

Factors	Level No	Contribution to the S/N
Soil Type	1.713	4.349
H_B/H_A Ratio	1.090	1.292
Damping Coefficient	0.922	1.918
Number of Damper	0.624	0.573
Contribution of all factors		4.349
Expected value (S/N) / (m)		-42.408 / 131.95
Confirmation result (S/N) / (m)		-43.906 / 156.78
Confidence interval (α=95%) (S/N)		-44.576 – -40.240

Table 12. Contribution of the factors on the base shear forces of Structure B.

Factors	Level No	Contribution to the S/N
Soil Type	2.471	4.349
H_B/H_A Ratio	1.279	1.292
Damping Coefficient	0.650	1.918
Number of Damper	1.069	0.573
Contribution of all factors		5.469
Expected value (S/N) / (m)		-41.605 / 120,30
Confirmation result (S/N) / (m)		-44.210 / 162.37
Confidence interval (α=95%) (S/N)		-46.831 – -36.379

The average S/N effects for roof displacements of Structure A were given in Table 5. Fig. 4 represents the optimum conditions for the roof displacements of Structure A. According to Fig. 4, the parameters and their levels that minimize the maximum roof displacements were A1-B2-C2-D1. This means that the first level of soil type (no soil case), the second level of H_B/H_A ratio of 1.50, the second level of damping coefficient of viscous damper of $1x10^5$ N.s/m and the first level of number of damper (1 FVD) minimize the maximum roof displacements. In other words, the optimum conditions for the roof displacements of Structure A are the first level of soil type, the second level of H_B/H_A ratio, the second level of damping coefficient of damper and the first level of the number of damper. The contribution of the factors on the roof displacements of Structure A and performance prediction are given in Table 9. The most effective factor on the roof displacements of Structure A is soil type, then damping coefficient of damper, then H_B/H_A ratio, and then the number of the damper. The average S/N effects for roof displacements of Structure B are given in Table 6. The optimum conditions for the roof displacements of Structure B are shown in Fig. 5. According to Fig. 5, the parameters and their levels that minimize the maximum roof displacements are A1-B1-C2-D1. This means that the first level of soil type (no soil case), the first level of H_B/H_A ratio of 1.00, the second level of damping coefficient of viscous damper of $1x10^5$ N.s/m and the first level of number of damper (1 FVD) minimize the maximum roof displacements. The contribution of the factors on the roof displacements of Structure A and performance prediction is given in Table 10. The most effective factor on the roof displacements of Structure B is H_B/H_A ratio, then soil type, then the damping coefficient of damper, and then the number of the damper.

The average S/N effects for base shear forces of Structure A are given in Table 7. Fig. 6 represents the optimum conditions for the base shear forces of Structure A. According to Fig. 6, the parameters and their levels that minimize the maximum base shear forces are A1-B2-C2-D1. This means that the optimum conditions for the base shear forces of Structure A are the first level of soil type, the second level of H_B/H_A ratio, the second level of damping coefficient of viscous damper, and the first level of the number of damper. The contribution of the factors on the base shear forces of Structure A and performance prediction is given in Table 11. The most effective factor on the base shear forces of Structure A is soil type, then H_B/H_A ratio, then the damping coefficient of damper, and then the number of the damper. The average S/N effects for base shear forces of Structure B are given in Table 8. Fig. 7 represents the optimum conditions for the base shear forces of Structure B. According to Fig. 7, the parameters and their levels that minimize the maximum base shear forces are A1-B2-C2-D1. This means that the optimum conditions for the base shear forces of Structure B are the first level of soil type, the second level of H_B/H_A ratio, the second level of damping coefficient of viscous damper and the first level of the number of damper. The contribution of the factors on the base shear forces of Structure B and performance prediction is given in Table 12. The most effective factor on the base shear forces of Structure B is soil type, then H_B/H_A ratio, then the number of the damper, and then the damping coefficient of damper.

According to the results, the most effective factor and its level on the roof displacements and the base shear forces for both frames is the first level of soil type, i.e., rigid base (no soil) case. When taking the soil medium into account in the analysis, greater displacement and base shear force values were obtained. This is an expected result. However, the increase in the displacement and base shear force values became apparent when the soil got looser. In other words, as the soil gets stiffer, the displacement and base shear force values systematically decrease. This fact indicates that as the soil gets looser, greater amplification can be expected. It can be also said that, the effectiveness of viscous damper on response mitigation decrease when the soil gets looser. The H_B/H_A ratio has a minor effect on the roof displacements and base shear forces of Structure A, on the other hand, the H_B/H_A ratio is more effective on the response of Structure B which is the taller one. Minimum response is obtained when the H_B/H_A ratio is equal to 1.50 for both frames. Minimum roof displacements and base shear forces are obtained at the second level of the damping coefficient of viscous damper of $1x10^5$ N.s/m. These results correspond with those of the literature. The previous studies indicated that the optimum value of the viscous damper is the value that leads to the minimum response, although no optimization study has been carried out (Bhaskararao and Jangid 2004; Patel and Jangid 2014). Most of the previous papers indicated that the optimum value of the damping coefficient of dampers is between 10^5 and 10^6 N.s/m according to the characteristics of the problem handled in their studies (Xu et al. 1999; Zhang et al. 1999; Wu et al. 2017). The results also show that there is no necessity to interconnect every floor with dampers. Thus, more economical solutions can be obtained by using only one damper. At the optimum conditions, the decrease in the roof displacements and base shear forces of both frames were up to 30% relative to those of the reference system which is the unlinked system. The time histories of the roof displacements and the base shear forces are given in Figs. 8 and 9, respectively.

6. Conclusions

This paper presents optimum conditions for minimum system response of two adjacent frame structures interconnected by viscous dampers, including SSI effects. The optimum parameters were investigated for the adjacent structures-soil system which was subjected to seismic load by 2D FE analysis with the Taguchi method. An optimization study was carried out for soil type, height ratio of the frames, damping coefficient of viscous damper, and the number of viscous damper. According to the optimizations;

- It is determined that the most effective parameter on the system response was Soil Type.
- It can be said that viscous dampers are more effective in response mitigation in relatively stiffer soils.

- The minimum roof displacements and base shear forces were obtained at rigid base (no soil) case, 1.50 for the H_B/H_A ratio, 1x10^5 N.s/m for the damping coefficient of viscous damper, and 1 for the number of the viscous damper.
- When the soil medium is considered in the analysis, the minimum roof displacements and base shear forces were obtained at dense soil (Soil Type I) case, 1.50 for the H_B/H_A ratio, 1x10^5 N.s/m for the damping coefficient of viscous damper, and 1 for the number of the viscous damper.
- In order to obtain the minimum system response, it is sufficient that the damping coefficient of the viscous damper is equal to 1x10^5 N.s/m.
- There is no necessity to connect two neighboring frames by dampers on all floors. More economical solutions can be obtained by using only one damper.
- It is drawn that the Taguchi method can be applied with the FE method for determining optimum conditions of a soil-structure system for minimum system response.

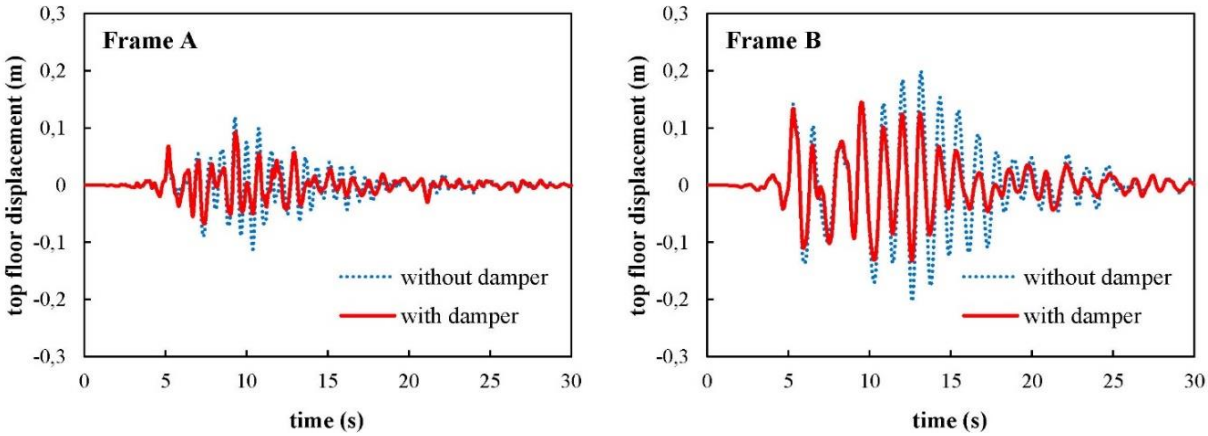

Fig. 8. Top floor displacement time histories at optimum conditions.

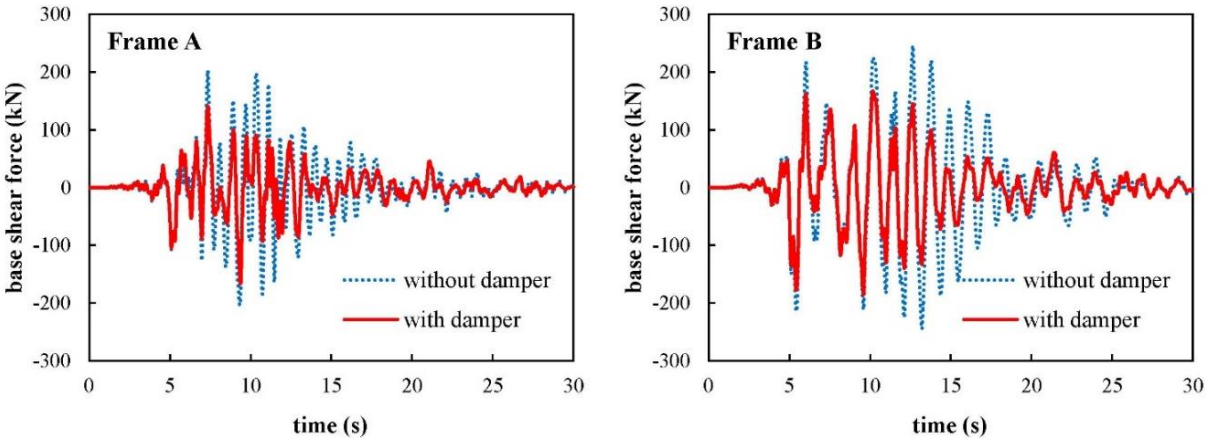

Fig. 9. Base shear force time histories at optimum conditions.

Acknowledgements

None declared.

Funding

The authors received no financial support for the research, authorship, and/or publication of this manuscript.

Conflict of Interest

The authors declared no potential conflicts of interest with respect to the research, authorship, and/or publication of this manuscript.

References

Ada M, Ayvaz Y (2019). The structure-soil-structure interaction effects on the response of the neighbouring frame structures. *Latin American Journal of Solids and Structures*, 16(8), 1-19.

ANSYS (2021). ANSYS Academic Research Mechanical (Version 19).

Avinash AR, Lingaraju MC, Kamath K (2017). Seismic performance of adjacent structures connected with Fluid viscous dampers by considering soil structure interaction-An analytical study. *International Journal of Civil Engineering and Technology*, 8(7), 421-431.

Bakre SV, Jangid RS (2007). Optimum parameters of tuned mass damper for damped main system. *Structural Control and Health Monitoring*, 14(3), 448-470.

Bayrak OÜ, Hınıslıoğlu S (2017). A new approach to the design of rigid pavement: single-axle loading. *Road Materials and Pavement Design*, 18(3), 573-589.

Bharti SD, Dumne SM, Shrimali MK (2010). Seismic response analysis of adjacent buildings connected with MR dampers. *Engineering Structures*, 32(8), 2122-2133.

Bhaskararao AV, Jangid RS (2004). Seismic response of adjacent buildings connected with dampers. *The 13th World Conference on Earthquake Engineering*, Vancouver, BC, Canada, Paper No. 3143, 1-14.

Bhaskararao AV, Jangid RS (2006a). Harmonic response of adjacent structures connected with a friction damper. *Journal of Sound and Vibration*, 292(3-5), 710-725.

Bhaskararao AV, Jangid RS (2006b). Seismic response of adjacent buildings connected with friction dampers. *Bulletin of Earthquake Engineering*, 4(1), 43-64.

Bhaskararao, AV, Jangid RS (2007). Optimum viscous damper for connecting adjacent SDOF structures for harmonic and stationary white-noise random excitations. *Earthquake Engineering and Structural Dynamics*, 36(4), 563-571.

Cimellaro GP, Garcia DL (2007). Seismic response of adjacent buildings connected by nonlinear viscous dampers. *Research Frontiers at Structures Congress*, Long Beach, California, United States, 1-12.

Çelebi E, Göktepe F, Karahan N (2012). Non-linear finite element analysis for prediction of seismic response of buildings considering soil-structure interaction. *Natural Hazards and Earth System Sciences*, 12, 3495-3505.

De Domenico D, Ricciardi G, Takewaki I (2019). Design strategies of viscous dampers for seismic protection of building structures: a review. *Soil Dynamics and Earthquake Engineering*, 118, 144-165.

Düzgün OA, Hatipoğlu YS (2022). Effective damping coefficient of fluid viscous dampers for dynamic response mitigation of coupled frames. *Journal of Vibration Engineering and Technologies*, Article in Press.

Hou CY (2008). Fluid dynamics and behavior of nonlinear viscous fluid dampers. *Journal of Structural Engineering*, 134(1), 56-63.

Housner GW, Bergman A, Caughey TK, Chassiakos AG, Claus RO, Masri SF, Skelton RE, Soong TT, Spencer BF, Yao JTP (1997). Structural control: past, present, and future. *Journal of Engineering Mechanics*, 123(9), 897-971.

Luco JE, De Barros FCP (1998). Optimal damping between two adjacent elastic structures. *Earthquake Engineering and Structural Dynamics*, 27(7), 649-659.

Lysmer J, Kuhlemeyer RL (1969). Finite dynamic model for infinite media. *Journal of the Engineering Mechanics Division,* 95(4), 859-878.

Makris N, Constantinou MC (1990). Viscous dampers: testing, modeling and application in vibration and seismic isolation. *National Center for Earthquake Engineering Research, Technical Report (NCEER-90-0028)*, State University of New York at Buffalo, New York, United States.

Patel CC, Jangid RS (2008). Influence of Soil-structure Interaction on Response of Adjacent SDOF Structures Connected by Viscous Damper. *The 12th International Conference of International Association for Computer Methods and Advances in Geomechanics*, Goa, India, 1-6.

Patel CC, Jangid RS (2014). Dynamic response of identical adjacent structures connected by viscous damper. *Structural Control and Health Monitoring*, 21(2), 205-224.

Taguchi G (1960). Table of orthogonal arrays and linear graphs. *Reports of Statistical Application Research*, 6, 1-52.

Tezcan SS, Uluca O (2003). Reduction of earthquake response of plane frame buildings by viscoelastic dampers. *Engineering Structures*, 25(14), 1755-1761.

Tubaldi E, Barbato M, Dall'Asta A (2014). Performance-based seismic risk assessment for buildings equipped with linear and nonlinear viscous dampers. *Engineering Structures*, 78, 90-99.

Tubaldi E (2015). Dynamic behavior of adjacent buildings connected by linear viscous/viscoelastic dampers. *Structural Control and Health Monitoring*, 22(8), 1086-1102.

Uz ME (2009). Improving the Dynamic Behaviour of Adjacent Buildings by Connecting Them with Fluid Viscous Dampers. *M.Sc. thesis*, School of Civil, Mining and Environmental Engineering, University of Wollongong, Wollongong, Australia.

Westermo BD (1989). The dynamics of interstructural connection to prevent pounding. *Earthquake Engineering and Structural Dynamics*, 18(5), 687-699.

Wolf JP (1988). Soil-Structure Interaction Analysis in Time Domain. Prentice Hall, New Jersey, United States.

Wu QY, Zhu HP, Chen XY (2017). Seismic fragility analysis of adjacent inelastic structures connected with viscous fluid dampers. *Advances in Structural Engineering*, 20(1), 18-33.

Xu YL, He Q, Ko JM (1999). Dynamic response of damper-connected adjacent buildings under earthquake excitation. *Engineering Structures*, 21(2), 135-148.

Zhang W, Xu Y (1999). Dynamic characteristics and seismic response of adjacent buildings linked by discrete dampers. *Earthquake Engineering and Structural Dynamics*, 28(10), 1163-1185.

Zhu H, Wen Y, Iemura H (2001). A study on interaction control for seismic response of parallel structures. *Computers and Structures*, 79(2), 231-242.

Zhu HP, Xu YL (2005). Optimum parameters of Maxwell model-defined dampers used to link adjacent structures. *Journal of Sound and Vibration*, 279(1-2), 253-274.

Zou L, Huang K, Wang L, Butterworth J, Ma X (2012). Vibration control of adjacent buildings considering pile-soil-structure interaction. *Journal of Vibration and Control*, 18(5), 684-695.